



Behaviour of circular footings confined by rigid base and geocell reinforcement

Pezhman Fazeli Dehkordi¹ · Usama Farhan Abdul Karim²

Received: 8 April 2020 / Accepted: 6 October 2020 / Published online: 16 October 2020
© Saudi Society for Geosciences 2020

Abstract

Soil in nature may exist in a stratified state. A possible condition is the case of a rigid layer underlying a weak sand stratum. In this instance, the bearing capacity of a shallow footing is affected by the lower rigid boundary. The treatment of thin soil layer by geocell reinforcement to raise the load carrying capacity of single shallow footing has been limited in the literature. Accordingly, rigid base and geocell reinforcement are investigated separately and in combination to study their influence on the behaviour and BC of shallow circular footings in dry sand bed. To capture that effect, different size rigid circular footings were tested on a bed in fully instrumented small- and large-scale laboratory installations. The ratio of sand layer thickness to footing diameter was changed considering optimum dimension and embedment depth for geocell mattress. The extensive laboratory part involved monitoring subgrade deformations, soil-geocell stresses and strains revealing the appropriate models for failure mechanisms in the presence of such confinements. Large increase in bearing capacity up to 225% and significant settlement reduction up to 66% are measured for the combined case. Base confinement less than three times the footing diameter in combination with the geocell mattress resulted in favourable higher design performance factors. New equations are proposed to estimate these factors for design and to extend classical formulations for footings strengthened by combined geocell-base confinement. A design performance factor is dependent on footing diameter, sand relative density and the ratio of layer thickness to footing diameter. As this ratio increases, this design factor decreases reaching a constant value at the critical depth.

Keywords Bearing capacity and settlement · Geocell reinforcement · Circular footing · Rigid base · Footing size

Introduction

First-generation bearing capacity (BC) equations (Terzaghi 1943) require some modifications for any boundary effects. In many practical situations, a thin sand layer is underlain by hard stratum such as bedrock. The presence of a stiff stratum within a certain depth beneath weak sand layer supported the footing base results in vertical confinement and can notably

affect the sand bearing pressure (Meyerhof 1974; Tournier and Milović 1977; Pfeifle and Das 1979; Brown et al. 2004; Cerato and Lutenecker 2006; Eid et al. 2009).

On the other hand, using 3D honeycombed reinforcement such as geocell to stabilise loose soils BC has grown significantly in recent years due to its effect to increase vertical and creating lateral confinement. Load-settlement behaviour and BC enhancement of the footings in low-bearing soils by the geocell reinforcement (GR) is cited in the past and more recent investigations (e.g. Dash et al. 2003a, b; Zhou and Wen 2008; Pokharel et al. 2010; Moghaddas Tafreshi et al. 2014, 2015; Lal et al. 2017; Hegde 2017; Shadmand et al. 2018; Tavakoli Mehrjardi et al. 2019).

Both confinement results in containment and reduction of soil deformations within the foundation influence zone. Enhancement is to be seen as higher load carrying capacity at the same displacement, lower displacement at the same load or both. Assessment of settlement and BC enhancement is required when a design entails including rigid horizontal and (or) flexible boundary layers. The stiffening effect from the

Responsible Editor: Zeynal Abiddin Erguler

✉ Pezhman Fazeli Dehkordi
p_fazeli@iaushk.ac.ir

Usama Farhan Abdul Karim
u.f.a.karim@utwente.nl

¹ Department of Civil Engineering, Shahrekord Branch, Islamic Azad University, Shahrekord, Iran

² Faculty of Technology, University of Twente, Enschede, The Netherlands

confinement eliminates the need to enlarge foundation dimensions and replace in situ weak soils. There is presently little guidance, however, on how to account for these boundaries dimensional and martial parameters as part of design iterations to obtain corrected allowable loads and corresponding safe settlements. Results from researches similar to above-mentioned may be appropriate in the countries near coastline that consists of sea-bed cohesionless deposits that are underlain by sandstone supporting the several giant buildings.

In this laboratory investigation on circular footings, the bearing soil is poorly graded sand and confinement is imposed from a rigid base (RB) and an embedded GR mat. Interference from any relative stiffness layer than the bearing soil results in complex soil-structure interactions that cannot be accommodated by an explicit shear mechanism. The separate or combined effect from such interaction often obscures defining an overall BC failure load (Bush et al. 1990). Modified BC for such combination was reported first by Fazeli Dehkordi et al. (2019a, b) to gain the interference factor of two closely spaced footings in the condition of three confinement types from RB, GR and the effect of existing second footing. Fazeli Dehkordi et al. (2019a, b) were focused on the modifications of interference factor due to the spacing between footings at different confinement conditions. Introducing a second footing is also equivalent to surface confinement to upward deformations and tensile stresses for which sands have no resistance. No analytical or limit-state plasticity type solutions can be derived for the actual slip mechanisms created by the combined confinements. The unique slip mechanisms may be discontinuous and cannot be generalised to produce universally applicable solutions (Bush et al. 1990). Hence, for all the cases investigated, an experimental setup is used whereby enhanced BC and settlement behaviours are recorded to determine new performance factors associated with the problem materials and geometric parameters. These factors are estimated in this study for single footings from their load-deformation behaviours in the presence or absence of RB and GR up or close to collapse. From the same tests, it is also possible to estimate settlement reduction factors. In the field, this combined effect of GR and the RB is of practical interest in relatively low density sands when an RB is close enough to affect but not fulfil design requirements for higher BC and smaller settlements. This and the earlier study on twin footings show that such modified BC-settlement performance factors can be retrieved from the experimental tests on RB-GR-confined soils. With the instrumented tests on two different size discs, this investigation provides new dimensionless relationships for the design of circular footings on GR sand layers of limited and infinite thickness.

This paper investigates, using instrumented small and large test-scale circular footings, the benefits in BC-settlement response gained from separated and coupled confinement by a GR and a RB for a single isolated footing. A method termed

here “design performance factors (DPF) method”, based on extensive laboratory testing, is explained to (i) evaluate the beneficial effects of BC increase and decreased settlement from RB and GR; (ii) elucidate the failure mechanism by monitoring subgrade deformation, pressure transmitted to the soil bed and strain generated in the GR to expand classical relationships for computing BC of encased soils; (iii) investigate the effect of footing size on the result trend of this study.

Experimental setup and program

Experimental setup (Fig. 1) with material (geocell/sand) property dimensions and program (Tables 1, 2 and 3) are given in this section. The sand-filled geocell is a commercial type HDPE mattress with perforated roughened cells arranged in regular horizontal rows welded together in a honeycomb.

Plate load tests on unreinforced and GR sand were performed in an instrumented square steel box of 1400 mm height with rough concrete base, fabricated from thick plates stiffened by steel belts for rigidity (Fig. 1). The setup ensured that the box should be large enough compared with the footing diameter such that its boundaries do not influence the footing response. A square test box with 2400 × 2400-mm plan dimensions was used to house all test components. Rigid steel plates with a rough base, 30 mm thick and 400 mm diameter were used, of approximately twice the equivalent diameter of one cell pocket of the GR, so that all the GR cell walls can fall under the footings’ periphery. The dimensions of test box were in conformity with those offered by Ueno et al. (1998) for large-scale circular footings. The sand was laid down in the model tank, and the hammer with size of 150 × 150 mm was used to compact sand bed and keeping the target relative density (15.62 kN/m³). Each layer is 100 mm thick to reach the elevation required for the reinforcement to be laid. Similar method is also used to compact infill sand in GR till the level of the GR is reached in terms of $u/B = 0.1$. During testing, the load remained central and entirely vertical applied through by a manually operated hydraulic jack fixed to the reaction frame and loading arm pinned to the footing via a load cell. Displacement was measured from two LVDTs (linear variable differential transformers) connected to data logger at diametrically opposite edges of the footing. A settlement ratio corresponding to $S/B = 2\%$ is used to determine the BC. This is allowable serviceability settlement limit, according to Meyerhof (1974). BCs are also identified for $S/B = 10\%$ settlements which were considered as ultimate pressures.

The small-scale tests, box with 900 × 900 mm widths in plan and 700 mm height, were also manufactured and given in Fig. 1 and Table 2. Rigid plastic of circular shape with 100 mm thickness and 150 mm diameter was used as the footing. This footing diameter is smaller than the equivalent diameter of one pocket cell of the GR and completely locates

Table 1 Materials characteristics

| Properties of sand | | Properties of GR | |
|--|-------|---|--------------|
| Classification | SP | Geocell material | Polyethylene |
| Medium particle size, D_{50} (mm) | 0.25 | Size of cell (mm) | 250 × 210 |
| Uniformity coefficient, C_u | 1.65 | Height of cell (mm) | 150 |
| Curvature coefficient, C_c | 0.84 | Thickness of strip (mm) | 1.5 |
| Max void ratio, e_{max} | 0.91 | Density (g/cm ³) | 0.94 |
| Min void ratio, e_{min} | 0.53 | Short-term yield resistance (kN/m) | 21 |
| Dry unit weight, γ_d (kN/m ³) | 15.62 | Elastic modulus (MPa) | 270 |
| Friction angle, φ^a (degree) | 36 | Perforation-cell wall (mm) | 10 |
| Specific gravity, G_s | 2.63 | Cell area (mm ²) | 26,200 |
| Relative density D_r (%) | 68 | Equivalent cell diameters ^b , d (mm) | 183 |
| Void ratio | 0.652 | Total open area of the cell wall (%) | 16 |

^a From ASTM standards; φ is average of 3 triaxial drained tests

^b $A = \pi d^2 / 4$

inside a cell without the presence of cell walls beneath the footings. The small footing diameter (150 mm) with footprint smaller than one pocket cell of the GR may lead to local effects according to Rajagopal et al. (1999). The presented results of small-scale tests are helpful to understand the basic mechanism and overall trends in the results. The results of small- and large-scale tests can also be extrapolated to full-scale models by careful consideration of scaling laws (Butterfield 1999). Other conditions of small-scale models were the same as for the larger-scale tests.

Table 2 shows dimensionless factors for the large and small model test. The chosen u/B and b/B dimensions are consistent with optimal values based on Dash et al. (2001). The geocell height is optimum according to Oliaei and Kouzegaran (2017) when $0.3 < h/B < 0.4$. Therefore, the ratio of h/B is optimum for the large model tests. The d/B ratios have no optimum values since the GR is of constant cell dimension.

Axial strains produced in the geocell mattress in the large-scale tests were measured and recorded, respectively, by a calibrated small strain gauge and data-logger network as described. The strain gauge with 120 Ω electrical resistances and 10 mm gauge length was calibrated by a tensile testing machine for a wide range of loads. Geocell surfaces are roughened using sand paper, cleaned and the strain gauge is glued in the horizontal direction on the outer surface of the geocell at mid height of the cell wall below the footing centre line. A

small size pressure cell with steel diaphragm and 50 mm diameter calibrated by fluid pressure is used below the geocell mattress under the footing centre and pocket opening of geocell to estimate the distributions of the vertical stress on the subgrade sand. Using a digital data logger, data from the pressure cell are also recorded.

Testing consisted of 18 tests as shown in Table 3. The RB depth H in each experiment is fixed as given in Table 3. Repeatability tests on GR and unreinforced bed resulted in only 3–6% deviations in BC. Small-scale tests up to $H/B = 4$ ensured sufficient range to cover a critical influence depth for rigid boundary. Furthermore, these tests were done for $H/B \geq 2$ on reinforced bed due to required space for GR height.

Non-dimensional performance indicators

For the RB confinement, Mandel and Salençon (1972) and Meyerhof (1974) proposed the modified BC (N_{γ}^*) and shape (S_{γ}^*) factors, respectively. These factors were presented in charts in terms of the bearing layer friction angle (φ) and thickness to footing width ratio (H/B). Meyerhof (1974) proposed the following BC equation valid for an influence zone of $H/B \leq 1$ for rectangular and circular footings. For a soil of unit weight γ :

Table 2 Dimensionless factor of geocell configuration

| Footing diameter (mm) | Footing thickness (mm) | Footing material | u/B | d/B | h/B | b/B | d/h | d/D_{50} |
|-----------------------|------------------------|------------------|-------|-------|-------|-------|-------|------------|
| $B = 150$ | 100 | Plastic | 0.1 | 1.22 | 1 | 4 | 0.82 | 732 |
| $B = 400$ | 30 | Steel | 0.1 | 0.46 | 0.38 | 4 | 0.82 | 732 |

u thickness of sand cover on the geocell, b geocell width, h geocell height, B footing diameter, d equivalent diameter of geocell opening pocket, D_{50} medium sand grain size

Table 3 Test details

| Test series | Footing width | Reinforcement type | H/B | Test number | Aim |
|-------------|---------------|--------------------|-----------------|--------------------|---|
| 1 | B = 400 mm | Unreinforced | 0.5, 1, 2, 3 | 4 + 1 ^a | To assess the influence of H/B |
| 2 | B = 400 mm | GR | 1, 2, 3 | 3 + 1 ^a | To appraise the influence of H/B and the GR |
| 3 | B = 150 mm | Unreinforced | 0.5, 1, 2, 3, 4 | 5 | To study the effect of footing size and H/B |
| 4 | B = 150 mm | GR | 2, 3, 4 | 3 + 1 ^a | To evaluate the effect footing size, GR and H/B |

^a To verify the repeatability of the test data, the tests were conducted two times

$$q_u = 0.5\gamma BN_\gamma^* S_\gamma^* \tag{1}$$

where

$$S_{\gamma\text{circle}}^* = 1 - m_2 \left(\frac{B}{L} \right) \tag{2}$$

where S_γ^* is the shape factor of circular footing in confined soil, m_2 is the function of H/B and φ , and L is the footing length. For $H/B \geq 1$, Meyerhof (1974) proposed $N_\gamma^* = N_\gamma$ and $S_\gamma^* = 0.6$ for circular footings which is the same as that suggested by Terzaghi for an unbounded layer. Cerato and Lutenegger (2006) using plate tests on the sand at different densities concluded that the modification as in Eq. (1) is valid up to $H/B \geq 3$ recommending $S_\gamma^* = 0.6$ for bounded layers.

To account for shape effect for a circular footing, the following equation is suggested for multiple confinements from RB and GR:

$$q_u = 0.5\gamma BR_\gamma K_\gamma (N_\gamma S_\gamma) \tag{3}$$

where K_γ and R_γ are, respectively, the RB and GR correction factors which are design performance factors.

To facilitate plotting experimental results and evaluate the separate and combined effects of GR and base layers, BC (BCR) and settlement (PRS) performance indicators (non-dimensional ratios) are defined. The BCR is defined as

$$BCR = \frac{q_{u\text{-Rein.b}}}{q_{u\text{-Unrein.b}}} \tag{4}$$

where $q_{u\text{-Unrein.b}}$ = footing BC for unreinforced sand overlying the RB; $q_{u\text{-Rein.b}}$ = BC for GR sand overlying the RB on the same footing and settlement.

To measure the GR effect on footing settlement, a percentage reduction of settlement (PRS) ratio is given as

$$PRS = \left(\frac{S_{\text{Unrein.}} - S_{\text{Rein.}}}{S_{\text{Unrein.}}} \right) \times 100 \tag{5}$$

where $S_{\text{Unrein.}}$ = settlement of footing on unreinforced sand and corresponding to the footing BC in presence or absence of the RB; $S_{\text{Rein.}}$ = settlement of GR sand in the same arrangement and supporting the same footing corresponding to the BC of unreinforced sand.

Furthermore, a BC factor K_γ is defined to evaluate the influence of RB on the BC of unreinforced bed as

$$K_\gamma = \frac{N_\gamma^* S_\gamma^*}{N_\gamma S_\gamma} \tag{6}$$

where $N_\gamma^* S_\gamma^*$ = footing BC factors on unreinforced sand overlying the RB, $N_\gamma S_\gamma$ = footing BC factors on unreinforced sand without the RB.

Tests results: RB without GR

The pressure-settlement data are presented in Fig. 2 for test series 1 and 3. A clearly defined failure occurs only in the smaller footing due to nonlinear behaviour of the soil at greater pressures and punching type failure effect in the footings with smaller size. The BC corresponding to $S/B = 2\%$ is 105–149 kPa and 45–100 kPa for large- and small-scale model, respectively, while failure (BC corresponding to $S/B = 10\%$) occurs at pressures of 172 to 251 kPa and 137 to 301 kPa for large and smaller footing models, respectively, in which the largest BC and failure load take place at $H/B = 0.5$. By increasing H/B , the BC and the ultimate load become constant at approximately $H/B \approx 2$ and 3 in, respectively, larger and smaller footings tests. These values might be considered as limiting values for the RB effect, here named critical RB

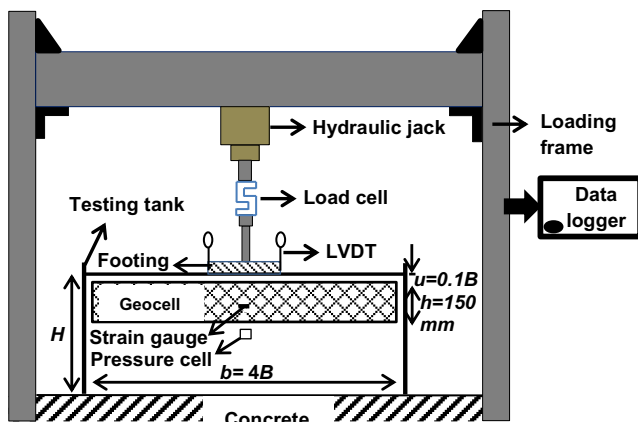


Fig. 1 Side view of experimental setup for large- and small-scale tests showing geocell, strain gauge and pressure cell locations

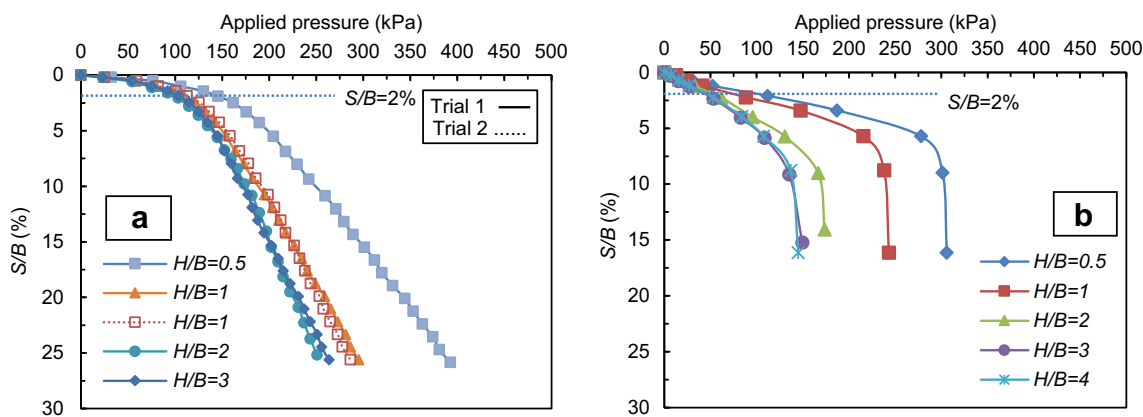


Fig. 2 Pressure-settlement plots—RB, no GR; a $B = 400$ mm, b $B = 150$ mm

depth. It is worth mentioning here that the critical depth of RB for larger footing is smaller and the difference between critical depths in both footings is significant. The difference between critical depths in both cases is due to the differences in the failure mechanism and shape of slip lines. On the other hand, the footing size directly affects the shape of failure mechanism and also depth of slip lines. Generally, BC of circular footing becomes constant in the literature at $H/B = 1.5-3$, depending on the relative density and soil characteristics.

Test results: RB with GR

The pressure-settlement response with GR is illustrated in Fig. 3. As expected, for the same foundation at the same H/B ratio, the BC with GR is always greater than without GR. Mostly, with the GR, no well-defined failure point is observed requiring interpolation. The slight reduction noted in pressure-settlement rate is due to distributing footing pressure by the GR over a larger area and linear behaviour of the geocell even at high pressure. Bending and shear resistance of the geocell support the sand beneath the footing even at higher

settlements (Han et al. 2008). Actually, geocell creates more confinement and prevents soil lateral movement resulted in greater load carrying capacity of the footing. The difference between critical depths for large and small size footings in the reinforced case is also significant. When $H/B = 1$ in large and $H/B = 2$ in small-scale tests, the BC value increases, respectively, 14% and 36% compared with those obtained from the cases without any confinements due to combined impact of the GR and RB.

As observed in the figure, the critical depth of RB is estimated at approximately $H/B = 2$ and $H/B = 3$ for large- and small-scale model tests, respectively, noting that the geocell does not substantially influence on critical depth compared with unreinforced cases.

The variation in BC and DPF at different H/B and settlement for footing on unreinforced as well as GR sand are reported in Table 4. For $H/B \geq (H/B)_{cr}$, the values given in Table 4 become nearly constant, stating that the RB has no serious influence beyond that depth. For determining K_γ and $R_\gamma K_\gamma$, the value of $H/B = 3$ and $H/B = 4$, respectively, for large and small footing is considered adequate to ensure that no rigid boundary effect below the footing can exist. DPF

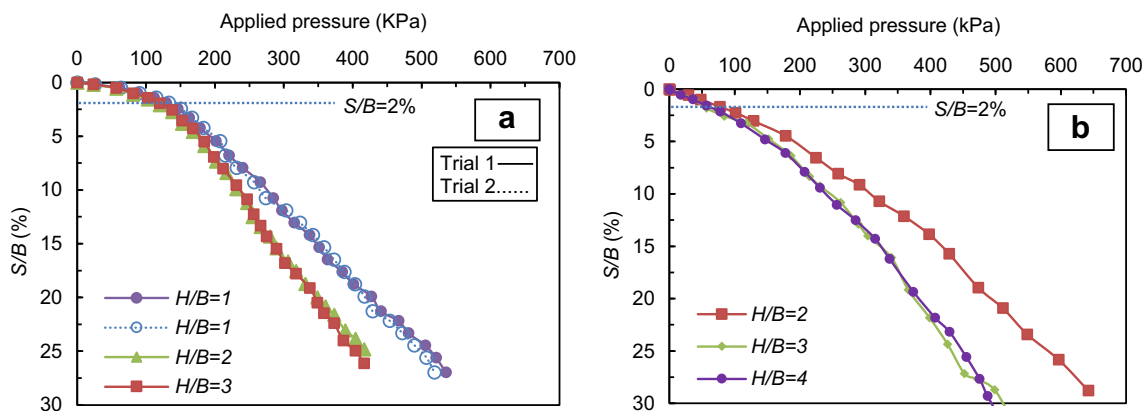


Fig. 3 Pressure-settlement plots—with GR; a $B = 400$ mm, b $B = 150$ mm

Table 4 BC and BC factors for different footing configurations

| Rein. Type | H/B | $B = 150 \text{ mm}$ | | | | | | $B = 400 \text{ mm}$ | | | | | |
|------------|-------|-------------------------|------------------------|---------------------------------|--------------------------|-------------------------|----------------------------------|-------------------------|------------------------|---------------------------------|--------------------------|-------------------------|----------------------------------|
| | | (BC) kPa $S/B = 2\%$ | $(K_\gamma) S/B = 2\%$ | $(R_\gamma K_\gamma) S/B = 2\%$ | (BC) kPa $S/B = 10\%$ | $(K_\gamma) S/B = 10\%$ | $(R_\gamma K_\gamma) S/B = 10\%$ | (BC) kPa $S/B = 2\%$ | $(K_\gamma) S/B = 2\%$ | $(R_\gamma K_\gamma) S/B = 2\%$ | (BC) kPa $S/B = 10\%$ | $(K_\gamma) S/B = 10\%$ | $(R_\gamma K_\gamma) S/B = 10\%$ |
| Unrein. | 0.5 | 100 | 2.22 | - | 301 | 2.20 | - | 149 | 1.45 | - | 251 | 1.46 | - |
| | 1 | 79 | 1.76 | - | 239 | 1.75 | - | 116 | 1.13 | - | 189 | 1.10 | - |
| | 2 | 58 | 1.29 | - | 168 | 1.23 | - | 103 | 0.98 | - | 172 | 1 | - |
| | 3 | 46 | 1.02 | - | 137 | 1 | - | 105 | 1 | - | 172 | 1 | - |
| | 4 | 45 | 1 | - | 137 | 1 | - | - | - | - | - | - | - |
| Rein. | 0.5 | - | - | - | - | - | - | - | - | - | - | - | - |
| | 1 | - | - | - | - | - | - | 138 | - | 1.31 | 274 | - | 1.59 |
| | 2 | 91 | - | 2.02 | 308 | - | 2.25 | 118 | - | 1.12 | 236 | - | 1.37 |
| | 3 | 64 | - | 1.42 | 232 | - | 1.69 | 121 | - | 1.15 | 236 | - | 1.37 |
| | 4 | 67 | - | 1.49 | 232 | - | 1.69 | - | - | - | - | - | - |

increases by increase of S/B , which shows more effectiveness of GR in larger settlements.

Failure mechanism

Soil deformation at failure of both type footings on unreinforced cases at various H/B values was measured in the tests. It was observed that soil climbing takes places around the footing due to ensuing general shear failure. The presence of RB near the footing interferes with failure surfaces and causes more complex stress distribution than in the reference case (without any confinements). In the GR tests, the sand could be confined between the GR and the bottom of the container. On the other hand, the conventional BC mechanism may change to squeezing. Figure 4 shows a probable failure mechanism of GR sand when the RB is located at a critical depth. Some researchers proposed to use a failure mechanism of shallow footing for the unbounded GR case (Dash et al. 2007; Pokharel et al. 2010).

Since no significant variation on the critical depth of RB was observed for reinforced compared with unreinforced shape of slip lines, the failure mechanism in GR sand is approximately the same as unreinforced bed. Heaving is prevented by GR not reaching ground surface (Fig. 4) due to bending and shearing resistance from GR. In this case,

negligible upward lifting is observed around the footing compared with unreinforced cases.

The width of sand zone undergoing uplift was measured for different sand layer thickness in unreinforced cases as plotted in Fig. 5. The figure reflects deeper and wider rupture surfaces in the smaller footing compared with the larger footing and the changed failure mechanism shape. Increase in the H/B ratio will therefore increase the width of rupture surfaces.

BC and settlement performance indicators

DPF (K_γ and $R_\gamma K_\gamma$)

To consider the influence of RB and GR on the BC, by the results of Table 4 for service load, two equations were interpolated to determine DPF for, respectively, unreinforced as well as GR sand, as indicated in Eqs. (7) and (8).

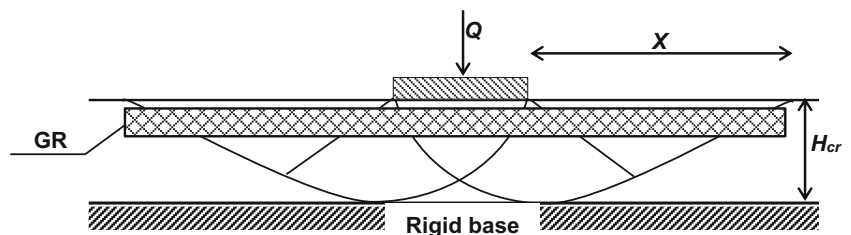
$$K_\gamma = -0.15(H/B)^3 + 0.92(H/B)^2 - 1.85(H/B) + 2.17 \quad (7)$$

$$R_\gamma K_\gamma = 0.11(H/B)^2 - 0.52(H/B) + 1.72 \quad (8)$$

where H = layer thickness beneath footing, B = footing width.

These interpolations have been carried out by fitting curve with correlation coefficient of $R^2 = 0.98$ using Matlab (2015) software which shows good accuracy for geotechnical

Fig. 4 Failure mechanism proposed for footing on finite sand layer overlaying RB at critical depth in GR bed



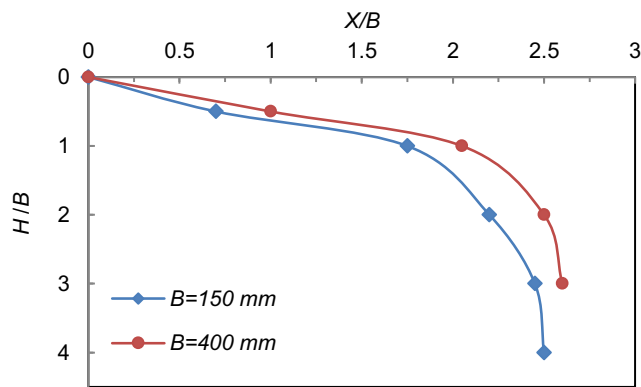


Fig. 5 Variation of H/B in terms of X/B for large- and small-scale footings placed on unreinforced sand

engineering purpose. Also, these equations are defined based on two main parameters, including layer thickness beneath the footing and the footing width (H/B) in which both have a significant effect on the footing BC and settlement. By determining K_γ and $R_\gamma K_\gamma$ from above formulation, the footing BC can be estimated by Eq. (3) for allowable settlement which is practical load.

Most previous equations presented to determine footing BC on GR sand was defined by the analytical method (Presto 2008; Koerner 2012; Avesani Neto et al. 2013) without considering RB effect. In the previous studies, the GR effect was examined by adding a sentence to the classical BC equations. The BC is determined as a function of applied pressure over the ground surface and the footing width (B) is not seen directly in the formulation. Commonly, in the analytical solutions, one or three mechanisms for calculation of BC due to GR were considered including “confinement effect”, “load dispersion effect” and “membrane effect”.

Increasing in the confining pressure due to applied stress on GR footing bed leading to dissipating the load through lateral direction tends to mobilise shear stress between geocell and infill soil shearing stress among adjacent cells and increasing infill soil deformability and stiffness called confinement effect. Spreading pressure underlying geocell mattress due to distributing stress over the larger area leading to reduce stress level beneath reinforcement called load dispersion effect. The membrane effect occurs due to vertical displacement in the footing soil under the geocell layer, which creates a concave shape in the tensioned geocell material.

Table 5 shows a comparison between the results of the present study for large-scale footing with those obtained from others using analytical approaches. For comparison, the value of $H/B = 3$ is used as a layer with infinite thickness. All sand properties and geocell geometry were assumed the same in all studies. As can be observed, the results of the present study have good compatibility with other investigations. Applied pressure defined in the equations of Table 5 is corresponding to the $S/B = 2\%$ in the pressure-settlement response.

Performance ratio BCR

Figure 6 presents the BCR variation in terms of S/B at different H/B values for a large- and small-scale model. As seen, the GR has a significant effect on the BC especially, for higher S/B values. In smaller footings, lower S/B with slight slopes is contrasted with greater S/B for which the slope of BCR increases. The steep slope is observed for S/B more than 10% which can be related to further GR contribution to bearing pressures at higher S/B . In larger footings, BCR increases with smooth slope by increasing S/B . Combination of the RB and the GR in the larger footings tends to increase the BCR from 4 to 13% compared with the same models without RB for $S/B = 0-25\%$.

Settlement performance ratio PRS

The PRS values, according to PRS definition in Eq. (5) in service and ultimate load for small- and large-scale model tests are shown in Fig. 7. The results indicate that simultaneous effect of GR and RB tends to settlement reduction due to applied load, especially at greater load. The difference between large- and small-scale results can be attributed to scale effect.

Instrumentation

Figure 8 shows the measured strains in the larger-scale tests generated at the geocell wall for different values of H/B . Strains ranged 0–0.53% for footing pressures corresponding to $S/B = 0-25\%$ showing linear behaviour and enhanced contribution of GR at the higher pressure. Little buckling has been observed in geocell walls installed below footings. Buckling can affect strain gauge records. There appear to be greater buckling effect found in our tests at lower H/B . The usage of a close-by RB can cause more buckling in geocell walls and highly localised settlements, reducing GR effectiveness due to loss of bending and confinement. Besides, the interfacial soil-GR and membrane resistance are not mobilised.

The pressure cell records (P_u) were normalised with the applied pressure corresponding to the BC in unreinforced sand (q) at the service and ultimate load. Figure 9 shows P_u/q versus H/B for GR and unreinforced sand. In the absence of the RB, more than 44% reduction is observed in the pressure at 190 mm depth due to the presence of GR. This reduction reaches to 50% for $H/B = 1$ due to the influence of combined confinements.

Table 5 Summary of BC results on GR sand obtained from different equations

| References | Aim | BC equation | Calculation method and mechanism assumed | Description | BC kN/m ² |
|----------------------------|---------------------------------------|--|---|--|----------------------|
| Koerner (2012) | Effect of GR on BC | $q_u = CN_c S_c + qN_q S_q + 0.5\gamma BN_\gamma S_\gamma + 2P \tan^2(45-\varphi/2) \tan \delta$ | Anal. lateral dispersion effect | S_c, S_q, S_γ = shape factors N_c, N_q, N_γ = BC factors γ = soil unit weight (kN/m ³) B = footing width (m) q = surcharge load (kPa) c = soil cohesion (kPa) δ = interface shear angle between infill soil and the cell wall (degrees) φ = friction angle of geocell infill soil (degree) P = applied pressure on geocell (kPa) | 121.74 |
| Avesani Neto et al. (2013) | Effect of GR on BC | $q_u = CN_c S_c + qN_q S_q + 0.5\gamma BN_\gamma S_\gamma + [P - 4(h/d)K_0 P \tan \delta][BL / ((B + 2d)(L + 2d))]$ | Anal. confinement effect, lateral dispersion effect | h/d = geocell aspect ratio k_0 = coefficient earth pressure at rest δ = interface shear angle between infill soil and the cell wall (degrees) P = applied pressure on Geocell (kPa) c = soil cohesion (kPa) q = surcharge load (kPa) B = footing width (m) L = footing length (m) γ = soil unit weight (kN/m ³) S_c, S_q, S_γ = shape factors N_c, N_q, N_γ = BC factors | 107.25 |
| Present study | Combination effect of GR and RB on BC | $q_u = 0.5\gamma BN_\gamma S_\gamma R_\gamma K_\gamma$ $K_\gamma = -0.15(H/B)^3 + 0.92(H/B)^2 - 1.85(H/B) + 2.17$ $R_\gamma K_\gamma = 0.11(H/B)^2 - 0.52(H/B) + 1.72$ | Proposed method Exp. results | H = soil layer thickness B = footing width (m) γ = soil unit weight (kN/m ³) S_γ = shape factor N_γ = BC factor R_γ, K_γ = correction factors | 136.88 135.8 |

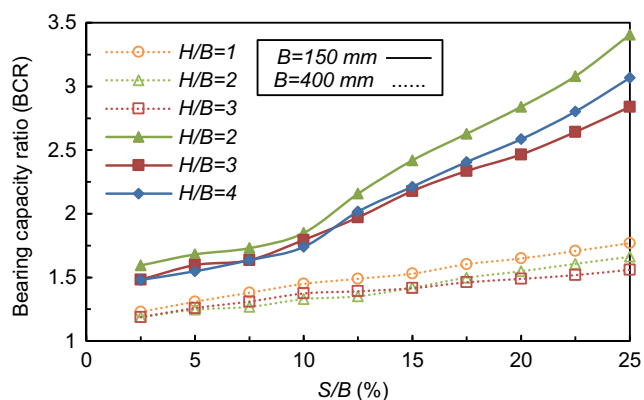


Fig. 6 Variation of BCR— S/B at different H/B

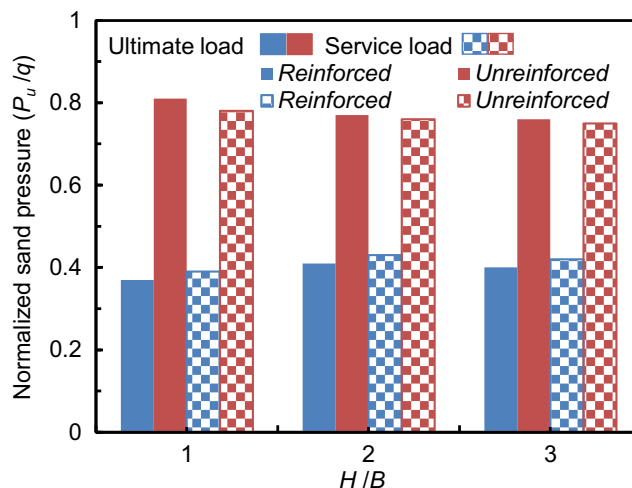


Fig. 9 Normalised pressure (p_u/q) versus H/B in large-scale tests for service and ultimate load

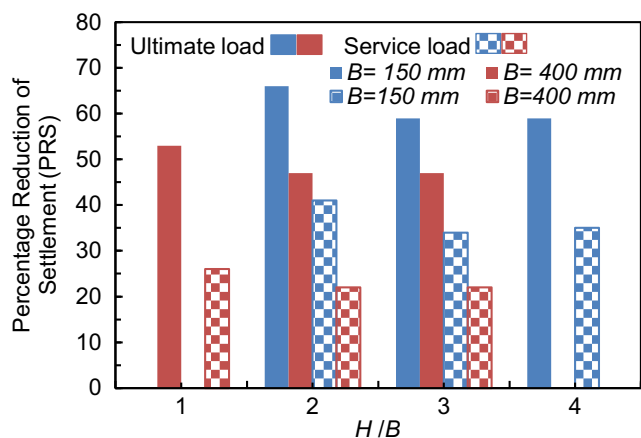


Fig. 7 Variation of PRS versus H/B for different footing sizes in service and ultimate load

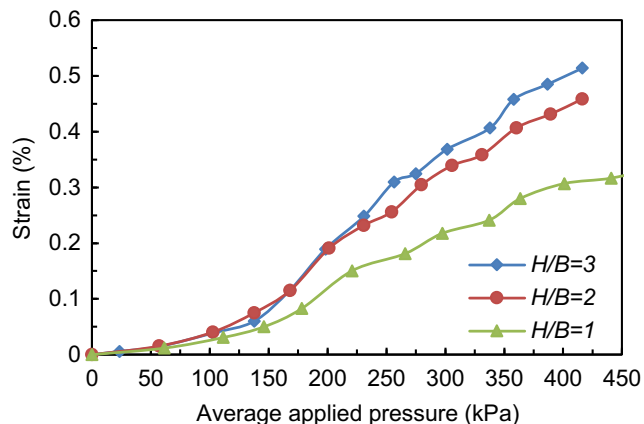


Fig. 8 Geocell wall strain produced in large-scale tests

Comparison

Figure 10 compares DPF for unreinforced cases (K_γ) obtained by back-calculation from Eq. (6) in allowable settlement ($S/B = 2\%$) with those given by theory and other experimental reports. As observed, a good agreement is seen between the current study and other results. The differences in the results with others are due to failure point determination methods, soil properties and footing size. For a small footing, punching type failure occurs and failure planes are deeper reaching the ground at low relative density (D_r). In the larger footing, rupture is less progressive along slip surfaces and lower average shear strength mobilised than for a smaller footing (De Beer 1965). In the larger footings, increased mean stress and decreased friction beneath the footing results from the curvature of Mohr-Coulomb failure line (Hettler and Gudehus 1988; Ueno et al. 1998; Zhu et al. 2001). Been and Jefferies (1985) stated that the combination influences of relative density, compressibility, mean stress, grain size and shape, and uniformity have a significant impact on the BC. The mean stress intensity in footings is also governed by the initial void

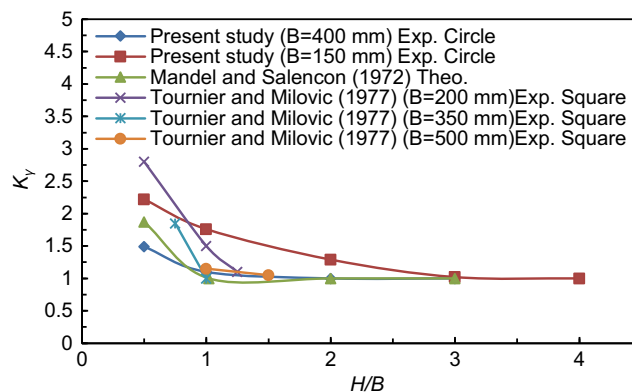


Fig. 10 Comparison of k_γ with other studies

Table 6 Comparison of BCR values for square and circular footings placed on GR sand

| Reference | Footing shape | Footing width/diameter (mm) | BCR ($S/B = 10\%$) | Description |
|-----------------------------|---------------|-----------------------------|----------------------|--|
| Shadmand et al. (2018) | Square | 500 | 1.57 | Test, SP, $\varphi = 41^\circ$, $D_r = 65\%$, EA (geocell) = 15 kN/m, $b/B = 5$, $d/B = 0.44$, $h/B = 0.3$, $u/B = 0.1$, $b/B = 4$ |
| Hegde and Sitharam (2013) | Square | 150 | 1.28 | Test, SP, $\varphi = 30^\circ$, $D_r = 65\%$, EA (geocell) = 21.5 kN/m, $d/B = 1.22$, $h/B = 1$, $u/B = 0.1$, $b/B = 5.9$ |
| Present study ($H/B = 3$) | Circle | 400 | 1.37 | Test, SP, $\varphi = 36^\circ$, $D_r = 68\%$, EA (geocell) = 21 kN/m, $d/B = 0.46$, $h/B = 0.38$, $u/B = 0.1$, $b/B = 4$ |
| Present study ($H/B = 3$) | Circle | 150 | 1.68 | Test, SP, $\varphi = 36^\circ$, $D_r = 68\%$, EA (geocell) = 21 kN/m, $d/B = 1.22$, $h/B = 1$, $u/B = 0.1$, $b/B = 4$ |

ratio and stress level relative to the critical state line (Cerato and Lutenege 2007).

The magnitude of BCR obtained from the present experiments is compared with values reported by others and presented in Table 6. Comparison is made for the $H/B = 3$ condition which indicates placing of the footing on the infinite layer. There is no data available in the literature wherein the footing BC can be determined using conventional methods for limited GR sand layer with different H/B ratios. As can be seen, the present values compare well with the experimental data available in the literature despite discrepancies in some cases. The differences may be attributed to material properties, GR type and footing shape.

Limitation and applicability

The results presented here are constrained by use of D_r value in the mid density range for this type sand (mentioned in Table 1), and GR specifications presented in Table 2. Although the results of the present study due to scale effect and several complex parameters may be partly different to full-scale footing performance in the field (Fakher and Jones 1996), the general behaviour can be expected to be similar (Milligan et al. 1986). Direct scaling up or down of the results for other material dimensional and material properties would not be appropriate, however due to non-linear effects. To increase geocell performance in practice, it is recommended to use smallest size cells at shallow depths of similar relative dimensions. Regarding the sand to be used at field scale, to provide scaling factors resulting from this study, the soil stiffness should be in the range for soils of similar average relative density and if feasible for low densities to increase it by compaction to arrive at similar relative density. GR makes sense to install at reasonable depths in soils with mid-range densities, not the low or the high stiffness soils. These findings can also be employed to guide geotechnical engineers for choosing appropriate parameters for foundation design located on GR sand. Other combinations can be tested in variety of ways

using this study and the DPF including physical and numerical modelling with results here employed as reference values bearing in mind the stated limitations.

Conclusions

Tests in small- and larger-scale experimental setups were carried out on two sets of circular footings supported by unreinforced and GR sand overlying a RB. The influences of RB location and GR on the footing pressure-settlement response were investigated in combination and separately. The behaviour of GR under vertical pressure in the presence and absence of the RB was elucidated monitoring GR strain and reduction stress intensity under the GR mat. The following conclusions may be drawn from the analysis:

- RB proximity shows greater BC and smaller settlement of footings generating different BC and DPF which are function of scale effect. When H/B ratio decreases to 0.5, the increase in the BC can reach to 225%.
- DPF is dependent on footing width (B), relative density (D_r), and dimensional ratios (H/B). As H/B increases, DPF decreases reaching to constant value (critical depth).
- GR in combination with RB in a thin packet of poorly graded sand, one footing diameter thick, can enhance BC by around 30 and 60% and improve settlement by around 25 and 50% under service and ultimate loads, respectively, compared with unreinforced infinite sand layer.
- The proposed equations (Eqs. (7) and (8)) can be used to estimate DPF and extend classical BC formulations as suggested by Eq. (3) for design of footings strengthened by GR and RB considering limitation and applicability.
- GR hardly affected BC and settlement performances when the RB is located at $3B$ and $2B$, respectively, below the small- and larger-scale footings. More research, however, is needed to be more conclusive on footing geometry (scale and shape) effects and sand relative density

(material) effects on BC and settlement performance factors.

Authors' contributions All authors contributed to the study conception and design. Material preparation, data collection and analysis were performed by Pezhman Fazeli Dehkordi. The first draft of the manuscript was written by Pezhman Fazeli Dehkordi and all authors reviewed and commented on previous versions of the manuscript. Usam F.A. Karim worked on conceptualization, review editing and project administration. All authors read and approved the final manuscript.

Data availability All data, models and code generated or used during the study appear in the submitted article.

Compliance with ethical standards

Conflict of interest The authors declare that they have no conflict of interest.

Code availability No code was developed or used in this research.

List of symbols b , Width of the geocell layer; B , Footing width; C , Soil cohesion; C_c , Curvature coefficient; C_u , Uniformity coefficient; d , Geocell pocket size; D_{50} , Medium grain size; D_r , Relative density; e_{max} , Maximum void ratio; e_{min} , Minimum void ratio; G_s , Specific gravity of soil; h , Height of geocell layers; H , Thickness of soil layer; H_{cr} , Critical thickness of soil layer; K_a , Active earth pressure coefficient; K_γ , Correction factor due to the RB; L , Footing length; m_2 , Constant factor; N_c , N_q , N_γ , Bearing capacity factors; N_γ^* , Modified bearing capacity factor; p , Applied pressure on geocell layer; P_{ur} , Pressure cell records; q , Applied pressure on the footing; q_{ur} , Ultimate bearing capacity; R , Fitting correlation coefficient; R_γ , Correction factor due to the GR; S_c , S_q , S_γ , Shape factors; S_γ^* , Modified shape factor; u , Geocell embedded depth; X , Rupture surface width for unreinforced sand; φ , Soil frictional angle; δ , Interface shear angle between the cell wall and the infill soil; γ , Soil unit weight; γ_d , Dry unit weight of the soil; σ_{vm} , Average vertical stress

Abbreviations BC, Bearing capacity; BCR, Bearing capacity ratio; DPF, Design performance factors; GR, Geocell reinforcement/reinforced; PRS, Percentage reduction of settlement; RB, Rigid base; SP, Poor graded sand

References

- Avesani Neto JO, Bueno B, Futai M (2013) A bearing capacity calculation method for soil reinforced with a geocell. *Geosynth Int* 20(3): 129–142
- Been K, Jefferies MG (1985) A state parameter for sands. *Géotechnique* 35(2):99–112
- Brown R, Valsangkar AJ, Schriver AB (2004) Centrifuge modeling of surface footings on a sand layer underlain by a rigid base. *Geotech Geol Eng* 22(2):187–198
- Bush DI, Jenner CG, Bassett RH (1990) The design and construction of geocell foundation mattresses supporting embankments over soft grounds. *Geotext Geomembr* 19(1):83–98
- Butterfield R (1999) Dimensional analysis for geotechnical engineers. *Géotechnique* 49(3):357–366
- Cerato AB, Lutenegeger AJ (2006) Bearing capacity of square and circular footings on a finite layer of granular soil underlain by a rigid base. *J Geotech Geoenviron Eng ASCE* 132(11):1496–1501
- Cerato AB, Lutenegeger AJ (2007) Scale effects of shallow foundation bearing capacity on granular material. *J Geotech Geoenviron Eng ASCE* 133(10):1192–1202
- Dash SK, Krishnaswamy NR, Rajagopal K (2001) Bearing capacity of strip footings supported on geocell-reinforced sand. *Geotext Geomembr* 19(4):235–256
- Dash SK, Sireesh S, Sitharam TG (2003a) Behaviour of geocell-reinforced sand beds under circular footing. *Ground Improv* 7(3): 111–115
- Dash SK, Sireesh S, Sitharam TG (2003b) Model studies on circular footing supported on geocell reinforced sand underlain by soft clay. *Geotext Geomembr* 21(4):197–219
- Dash SK, Rajagopal K, Krishnaswamy NR (2007) Behaviour of geocell-reinforced sand beds under strip loading. *Can Geotechn J* 44(7): 905–916
- De Beer E (1965) The scale effect on the phenomenon of progressive rupture in cohesionless soils. In *Proc 6th Int Conf Soil Mechanic Found Eng, Canada, Vol (2) No 3–6 pp: 13–17*
- Eid HT, Alansari OA, Odeh AM, Nasr MN, Sadek HA (2009) Comparative study on the behavior of square foundations resting on confined sand. *Can Geotechn J* 46(4):438–453
- Fakher A, Jones CJFP (1996) Discussion on bearing capacity of rectangular footings on geogrid reinforced sand. by Yetimoglu, T., Wu, J.T.H., Saglamer, A., 1994. *J Geotech Eng* 122:326–327
- Fazeli Dehkordi P, Ghazavi M, Ganjian N, Karim UFA (2019a) Effect of geocell-reinforced sand base on bearing capacity of twin circular footings. *Geosynth Int* 26(3):224–236
- Fazeli Dehkordi P, Ghazavi M, Ganjian N, Karim UFA (2019b) Parametric study from laboratory tests on twin circular footings on geocell-reinforced sand. *Sci Iran*. <https://doi.org/10.24200/SCI.2019.51471.2208>
- Han J, Yang X, Leshchinsky D (2008) Behavior of geocell-reinforced sand under a vertical load. *Transportation Research Record. J Transp Res Board* 2045:95–101
- Hegde A (2017) Geocell reinforced foundation beds-past findings, present trends and future prospects: a state-of-the-art review. *Constr Build Mater* 154:658–674
- Hegde A, Sitharam TG (2013) Experimental and numerical studies on footings supported on geocell reinforced sand and clay beds. *Int J Geotech Eng* 7(4):346–354
- Hettler A, Gudehus G (1988) Influence of the foundation width on the bearing capacity factor. *Soils Found* 28(4):81–92
- Koerner RM (2012) *Designing with geosynthetics*, vol 2, 6th edn. Xlibris Corporation, Lexington
- Lal D, Sankar N, Chandrakaran S (2017) Behaviour of square footing on sand reinforced with coir geocell. *Arab J Geosci* 10:345
- Mandel J, Salençon J (1972) Force portante d'un sol sur une assise rigide (étude théorique). *Géotechnique* 22(1):79–93
- Matlab (2015) Computer software. MathWorks, Natick
- Meyerhof GG (1974) Ultimate bearing capacity of footings on sand layer overlying clay. *Can Geotech J* 11(2):223–229
- Milligan GWE, Fannin RJ, Farrar DM (1986) Model and full-scale tests of granular layers reinforced with a geogrid. In: *Proc 3th Int Conf Geotext Vol 1*. Vienna, pp: 61–66
- Moghaddas Tafreshi SN, Khalaj O, Dawson AR (2014) Repeated loading of soil containing granulated rubber and multiple geocell layers. *Geotext Geomembr* 42(1):25–38
- Moghaddas Tafreshi SN, Shaghghi T, Tavakoli MehrJardi GH, Dawson AR, Ghadrnan M (2015) A simplified method for predicting the settlement of circular footings on multi-layered geocell-reinforced non-cohesive soils. *Geotext Geomembr* 43(4):332–344
- Oliaei M, Kouzegaran S (2017) Efficiency of cellular geosynthetics for foundation reinforcement. *Geotext Geomembr* 45(2):11–22
- Pfeifle TW, Das BM (1979) Bearing capacity of surface footings on sand layer resting on a rigid rough base. *Soils Found* 19(1):1–11

- Pokharel SK, Han J, Leshchinsky D, Parsons RL, Halahmi I (2010) Investigation of factors influencing behavior of single geocell-reinforced bases under static loading. *Geotext Geomembr* 28(6): 570–578
- Presto (2008) Geoweb load support system-technical overview. Presto Products Company, Appleton
- Rajagopal K, Krishnaswamy NR, Madhavi Latha G (1999) Behaviour of sand confined with single and multiple geocells. *Geotext Geomembr* 17(3):171–184
- Shadmand A, Ghazavi M, Ganjian N (2018) Load-settlement characteristics of large-scale square footing on sand reinforce with opening geocell reinforcement. *Geotext Geomembr* 43(3):319–326
- Tavakoli Mehrjardi G, Behrad R, Moghaddas Tafreshi SN (2019) Scale effect on the behavior of geocell-reinforced soil. *Geotext Geomembr* 47(2):154–163
- Terzaghi K (1943) *Theoretical soil mechanics*. Wiley, New York
- Tournier JP, Milović DM (1977) Étude expérimentale de la capacité portante d'une couche compressible d'épaisseur limitée. *Géotechnique* 27(2):111–123
- Ueno K, Miura K, Maeda Y (1998) Prediction of ultimate bearing capacity of surface footings with regard to size effects. *Soils Found* 38(3): 165–178
- Zhou H, Wen X (2008) Model studies on geogrid or geocell reinforced sand cushion on soft soil. *Geotext Geomembr* 26(3):231–238
- Zhu F, Clark JI, Phillips R (2001) Scale effect of strip and circular footings resting on a dense sand. *J Geotech Geoenviron Eng ASCE* 127(7):613–621